A fast charge-dependent atom-pairwise dispersion correction for DFTB3

Riccardo Petraglia[a], Stephan N. Steinmann[b] and Clemence Corminboeuf[a]*

[a]Laboratory for Computational Molecular Design, Institut des Sciences et Ingénierie Chimiques, Ecole Polytechnique Fédérale de Lausanne, CH-1015 Lausanne, Switzerland.

[b]Laboratoire de Chimie, Ecole Normale Superieure de Lyon, F-69364 Lyon, France

AUTHOR EMAIL ADDRESS clemence.corminboeuf@epfl.ch

Abstract

Organic electronic materials remarkably illustrate the importance of the "weak" dispersion interactions that are neglected in the most cost-efficient electronic structure approaches. This work introduces a fast atom-pairwise dispersion correction, dDMC that is compatible with the most recent variant of Self-consistent charge Density functional tight binding (SCC-DFTB). The emphasis is placed on improving the description of π-π stacked motifs featuring sulfur-containing molecules that are known to be especially challenging for DFTB. Our scheme relies upon the use of Mulliken charges using minimal basis set that are readily available from the DFTB computations at no additional cost. The performance and the efficiency of the dDMC correction are validated on series of examples targeting energies, geometries and molecular dynamic trajectories.

Introduction

The development of electronic devices based on π-conjugated polymers and oligomers[1–3] is driven by the opportunity to achieve novel functionalities (e.g. mechanical flexibility, transparency, impact resistance)[4–7] at reduced fabrication costs. The performance of such organic devices depends

heavily upon the organization of π-conjugated molecules or chains at the molecular level[3,8] and upon the electronic structure mirrored by the wavefunction. In this context, insightful structure-property relationships can be exploited if quantum chemistry is used concurrently with experiment. The main attractive interactions occurring between π-conjugated moieties arise from van der Waals forces that decay as R^{-6} at large intermolecular distances. The central role of computational approaches is hence to achieve an accurate description of London dispersion and establish how to fine-tune the relative displacements or orientations between π-conjugated cores. Despite their omnipresence, van der Waals interactions are not accounted for by standard semi-local and hybrid density functionals[9–11] that provide a practical balance of accuracy and computational cost unmatched by other methods. Over the last decade, tremendous efforts have been devoted to improving the description of dispersion forces within the DFT framework.[12,13] The most extensively used approaches consist in adding *a posteriori* an atom pairwise energy correction term (*vide infra*).[14–18] The various available pairwise schemes differ in the way the dispersion coefficients are obtained. For instance, Grimme's popular DFT-D is based only on pre-tabulated values,[17,19,20] the XDM model from Becke and Johnson computes the dispersion coefficients from the exchange-hole dipole moment,[21,22] Tkatchenko and Scheffler's vdW-TS connects the dispersion coefficients to the size of the atom in the molecule,[15] while their latest variant also accounts for the many-body physics.[23,24] Closer to the present context, Steinmann *et al.* formulated a classical[25] and density-dependent dispersion correction (dDsC),[18,26–28] which simplifies the computation of the XDM and exploits Hirshfeld (overlap) populations[29] to distinguish non-bonded regions from bonded atom pairs, eliminating the correction at covalent distances.[18]

The DFT framework as used in practice is convenient and efficient albeit restricted to systems made of few hundred atoms only. This limitation prevents the modeling of large-scale organic molecular materials. In comparison, tight binding and other semi-empirical approaches are capable of producing molecular geometries and energetics at dramatically reduced computational costs.[30] In particular, the Self-Consistent Charge Density Functional Tight-Binding (SCC-DFTB)[31] scheme, rooted within the DFTB method developed by Seifert *et al.*[32,33] as well as its most recent DFTB3

variant,[34–36] provide valuable insights and have already unraveled complex problems.[37–40] In the context of organic electronic materials, the novel parameterization for (bio)organic molecules (so called 3OB) is especially relevant as it restores the proper qualitative behavior[41,42] for molecules involving non-covalently bound sulfur atoms that were poorly described by the previous MIO11 parameter set.[43–45] Yet, SCC-DFTB suffers from the same deficiency as DFT functionals and does not account for dispersion interactions.[9,46] In this work, we propose a dispersion correction tailored for SCC-DFTB but inspired from the density-dependent dDsC correction. The proposed model is called dDMC due to its dependence on Mulliken charges[47] that are readily available from a SCC-DFTB computation. As such, dDMC does not require any additional information and is computationally very cheap. Alternative dispersion energy corrections adapted to SCC-DFTB/DFTB3 approaches exist. Elstner *et al.* proposed a method suitable for biological system that is based on the Slater-Kirkwood effective number of electrons.[9] Zhechkov *et al.* used the Universal Force Field London coefficients to correct the SCC-DFTB energy.[46] Rezac *et al.*, introduced the more sophisticated D3H4[48] method, which corrects for dispersion interaction using Grimme's D3[17] correction and improve the description of interactions involving hydrogen atoms. More recently, Grimme proposed a new parameterization of D3 specific for the DFTB3/3OB.[49] However, all these schemes have been parameterized and validated on biological systems with no specific consideration of typical π-π stacked molecules characteristics of organic electronics. The challenges associated with the modeling of these systems involve overcoming the interplay arising from the poor description of both the sulfur-containing moiteies[41,45] inherent to the DFTB parameters and the vdW interactions. The pragmatic dispersion correction proposed herein aims at providing efficiently reliable energies, geometries and molecular dynamic trajectories for sulfur-containing organic complexes. The next section describes the theoretical aspects of the dDMC that is followed by its validation.

Theory

dDMC is an *a posteriori* pairwise dispersion correction that adjusts the idea behind dDsC[18,25,26] to the simpler and less computationally expensive DFTB scheme.

The general approach to compute the dispersion energy is

$$E_{disp} = \sum_{i}^{N-1} \sum_{j>i}^{N} f_d(R_{ij}) \frac{C_{6,ij}}{R_{ij}^6} \quad (1)$$

The indexes i and j run over all the nuclei, R_{ij} is the internuclear distance, $C_{6,ij}$ is the dispersion coefficient associated with the interaction between the atom i and the atom j, f_d is a function that damps the correction at short internuclear distances that are better described by the DFTB Hamiltonian. The commonly used density-dependent schemes (e.g., XDM, dDsC) compute atomic dispersion coefficients from partitioning functions such as the Hirshfeld scheme. The same Hirshfeld partitioning is also used in the sophisticated damping function of dDsC. The simplification in dDMC aims at avoiding the computation of: i) integrals inherent to the Hirshfeld partitioning and ii) local density derivatives (i.e., the XDM) that are more demanding than SCC-DFTB itself. The Hirshfeld partitioning defines a weighting function:

$$w_i = \frac{\rho_i^{free}(\vec{r})}{\sum_j \rho_j^{free}(\vec{r})} \quad (3)$$

where $\rho_i^{free}(\vec{r})$ represents the electron density associated with the free atom *i* while $\rho(\vec{r})$ is the molecular electron density. The *j* index runs over all the atoms in the molecule.

One of the central quantities, on which density dependent dispersion corrections are based, is the estimate of the size of the atom in a molecule. In particular, the ratio between the volume of the AIM and the free atom:

$$\frac{V_i^{aim}}{V_i^{free}} = \left(\frac{\int r^3 w_i(\vec{r}) \rho(\vec{r}) d^3\vec{r}}{\int r^3 \rho_i^{free}(\vec{r}) d^3\vec{r}} \right) \quad (4)$$

can be conveniently approximated by Equation (5).

$$\frac{V_i^{aim}}{V_i^{free}} \simeq \frac{N_i}{Z_i} \qquad (5)$$

where N_i and Z_i are the Mulliken electronic population for the atom in the molecule and the number of electrons for the free atom i. This seemingly very crude approximation is motivated by a model of atoms with a uniform density inside the volume of the atoms. Our approach is correct in two limiting cases: i) the neutral, "free" atom and ii) when the atom has no electrons.

In 2009, Tkatchenko *et al.* linked the dispersion coefficient for an atom in a molecule ($C_{6,i}^{aim}$) to the dispersion coefficient of the free atoms ($C_{6,i}^{free}$) through the ratio displayed in eq. (4):[15]

$$C_{6,i}^{aim} = \left(\frac{V_i^{aim}}{V_i^{free}} \right)^2 C_{6,i}^{free} \qquad (6)$$

Directly exploiting our assumption we can define a new relation for the dispersion coefficient:

$$C_{6,i}^{aim} = \left(\frac{N_i}{Z_i} \right)^2 C_{6,i}^{free} \qquad (7)$$

We here discuss the results obtained with equation (7) with the $C_{6,i}^{free}$ available for most of the elements in the periodic table as provided by Grimme.[17]

We apply the same mixing rule as in our previous work[25] for the dispersion coefficients between atoms i and j.

$$C_{6,ij} = \frac{2C_{6,i}C_{6,j}}{C_{6,i} + C_{6,j}} \qquad (8)$$

It is important to stress that a dispersion correction based on the Mulliken scheme is ideally suited for SCC-DFTB. In contrast to large basis sets, small or minimal basis sets provide robust Mulliken charges.[50] In this respect, DFTB Mulliken charges (using minimal basis sets) are robust and very convenient since available at no cost in contrast to Hirshfeld charges (see details on the charges and on the C_6 coefficients in the Supplementary Materials).

The dDsC damping is based on the universal Tang and Toennies function[51,52] plus a second damping function with both depending on the information extracted from the electron density.

dDMC preserves the double damping and the flexibility of dDsC but without density-dependency and without adding extra cost to the electronic structure computation. In line with the "density dependent" approach, the damping function uses an electronic parameter to switch the correction on and off. The Fermi function[53] $F(a,s,R_{ij})$ damps a Tang and Toennies function $TT(b,R_{ij})$ to ensure enough flexibility

$$f_d(R_{ij},b) = F(a,s,R_{ij})TT(b_{ij}R_{ij}) \qquad (9)$$

The Fermi damping function

$$F(a,s,R_{ij}) = \frac{1}{1+\exp\left(-s\left(\frac{R_{ij}}{aR_{ij}^{vdW}}-1\right)\right)} \qquad (10)$$

contains an empirical parameter a that scales the van der Waals radii[54,55] ($R_{ij}^{vdW} = R_i^{vdW} + R_j^{vdW}$) and a steepness parameter s that minimizes the effect of the Fermi function at larger internuclear distances. The Tang and Toennies function is

$$TT(bR_{ij}) = 1 - \mathrm{e}^{(-b_{ij}R_{ij})}\sum_{k=0}^{6}\frac{(b_{ij}R_{ij})^k}{k!} \qquad (11)$$

in which the TT-damping factor (b_{ij}) regulates the medium range of the correction. b_{ij} is computed according to the combination rule

$$b_{ij} = 2\frac{b_i b_j}{b_i + b_j} \qquad (12)$$

The dDsC b_{ii} factor is defined as

$$b_i = b_0\sqrt[3]{\frac{1}{\alpha_i}} \qquad (13)$$

where b_0 is a fitted parameter and α_i is the polarizability of the interacting atoms in the molecule defined as $\alpha_i = \alpha_i^{free}\frac{V_i^{aim}}{V_i^{free}}$. Adopting the same idea to dDMC we get

$$b_{ii} = b_0\sqrt[3]{\frac{1}{\alpha_i}} = b_0\sqrt[3]{\frac{1}{\alpha_i^{free}}}\sqrt[3]{\frac{V_i^{free}}{V_i^{aim}}}\ ;\ b_0\sqrt[3]{\frac{1}{\alpha_i^{free}}}\sqrt[3]{\frac{N_i}{Z_i}} \qquad (14)$$

where the free atom polarizabilities (α_i^{free}) are taken from the CRC Handbook.[56]

This scheme and in particular the usage of a "double-damped" function ensures the right behaviour at both the short and medium/long range.

Note that akin to other dispersion corrections, -dDMC cannot solve the issues related to the poor description of H-bonded interactions by semi-empirical approaches.[57,58] Instead an additional empirical correction would be needed[48] for this purpose. However, our present objective is not to improve the description of H-bonds and increase the empiricism by adding a second correction but rather to provide a fast electronic structure scheme that accurately describes sulfur-containing compounds involved in pi-stacking interactions. Nevertheless, the proposed dDMC scheme could be further combined with a "H-bond corrections" to provide a more generally applicable scheme.

Gradient

The validation of the quality of the approximated gradients is essential in the context of both optimizations and molecular dynamic trajectories. Since the dispersion correction depends, through the Mulliken charges, on the electronic structure, the gradient has an electronic and a geometric contribution. To improve the computational efficiency, we neglect the electronic contribution, i.e., the Mulliken charges are fixed with respect to the atom displacements. In addition, given that the dispersion correction depends only on the interatomic distances, the gradients are computed directly in function of the distance instead of the coordinate's displacements:

$$F_{i,x} = -\sum_{j \neq i}^{N} \frac{\mathrm{d}(f_d(R_{ij}) C_{6,ij} R_{ij}^{-6})}{\mathrm{d}R_{ij}} \; ; \; -\sum_{j \neq i}^{N} \frac{\mathrm{d}(f_d(R_{ij}) R_{ij}^{-6})}{\mathrm{d}R_{ij}} C_{6,ij} \cdot \frac{\partial R_{ij}}{\partial x_i} \qquad (2)$$

where $F_{i,x}$ is the force acting on the atom i along the direction x. The validity of this approximation is verified through a comparison between the dispersion numerical gradients (computed using a displacement = 0.001 Å) and the approximated analytical ones on all the structures available in the S66 data set.[59] To enforce that gradient values are different from zero, a noise corresponding to a uniformly distributed random displacement comprised between -0.2 and 0.2 Å was added to the coordinates of all atoms. The Mean Average Error (MAE) computed as

$$\mathrm{MAE} = \frac{\sum_{i}^{N} |f_i - r_i|}{N} \quad (3)$$

using the numerical derivatives as reference values (r_i) and the approximated analytical gradients as forecast values (f_i) is 6.81×10^{-8} eV/Å on an absolute average dispersion force of 6.44×10^{-3} eV/Å. This implies that the error arising from the approximated analytical gradient is ~ 1×10^{-5} smaller than the average dispersion force arising from a deviation of 0.2 Å from the most stable configuration.

Adjustable Parameters and Training Set

The dDMC correction depends on two adjustable parameters, a and b_0, as well as on the steepness factor, s. In line with our former work,[25] the steepness factor, s = 46, was chosen such as to minimize the effect of the Fermi function on the overall damping at large internuclear separations by imposing the constraint $F(a,s,1.1 \cdot a \cdot R_{ij}^{vdW}) \geq 0.99$. Such a limitation turns the Fermi function off when the distance between the atoms (R_{ij}) is larger then $1.1 \cdot a \cdot R_{ij}^{vdW}$ so that only the $TT(b_0, r_{ij})$ damping is active in this region.

The two parameters, a and b_0, are trained for each electronic structure approach (the values are given in the SI) with the Nelder-Mead optimization method to reproduce a set of interaction energies. The training set includes a subset of the S66x8 data set[59] (namely the "dispersion" and "mixed" structures). To ensure a good performance on sulfur-containing compounds, the training set is completed with an expanded version of the Pi29n (i.e., Pi29nx8) that mimics the S66x8[59] data set adding 7 displaced structures for each dimer included in the original Pi29n.[60] For each structure, one scales the equilibrium distance between the monomers centre of mass (by 0.9, 0.95, 1.05, 1.10, 1.25, 1.50, 2.00). The interaction energies for each dimer (232 structures) are estimated at the CCSD(T)/CBS level[61,62] and corrected for BSSE using the Counter Poise (CP) correction[63] following the same scheme as used in the Pi29n data set.[60] The inclusion of energy profiles in the training phase serves to improve the response of the damping function at small intermolecular distance. To avoid issues arising from the self-interaction error, the charge transfer TTF-TCNQ

complex originally presents in the Pi29n data set[60] was not considered herein. In addition, since the emphasis is placed on improving the description of π-stacked motifs that are prevalent in organic electronic materials, we did not consider the hydrogen-bond complexes of the S66x8 data set. Note finally that the PM6 Hamiltonian[64] that was used for comparisons required the training of one additional scaling factor for the total dispersion energy.

Computational Details

All the computations are performed using a modified version of the ASE package[65] that applies the dDMC and D3 dispersion corrections to PM6 and DFTB3. The DFTB3 computations are performed using the DFTB+ 1.2.1 software[66] with the 3OB Slater-Koster files.[41,42] The Hubbard parameters, their derivatives as well as the γ factor are chosen according to Qui *et al.*[41,42]. PM6 computations were performed in MOPAC2012[67] with the default options. The D3 parameters are taken from Rezac *et al.*[48] and used with the software available from Grimme's website. The dDMC correction terms were computed using a standalone code that is distributed freely.

The ASE package delivers the QuasiNewton method to perform the geometry optimizations using homemade interfaces with the previous cited software. Optimizations are considered as converged if the forces on all individual atoms are below $5x10^{-3}$ eV/Å.

The Born-Oppenheimer molecular dynamics uses the implementation of the velocity Verlet algorithm in ASE to integrate the DFTB3/3OB and the corrected trajectories. The PBE-dDsC simulations are performed with a modified version of the QCHEM4.0 software package.[68]

The DFTB3/3OB simulations involving the dithiacyclophane molecule are performed in the NVE ensemble using a 0.5 fs time step in line with the PBE and PBE-dDsC trajectories obtained previously by Corminboeuf and co-workers.[69]. The starting structures were the same as in Ref. [69]. The initial temperature was set to 300 K. With this condition no energy drift has been observed. To ensure that the approximate gradients do not introduce instability in the MD trajectory, we used dithiacyclophane to verify what is the maximum time step that does not introduce an energy drift.

The drift was defined as the angular coefficient of the trendline that best fits the energy profile as a function of time. We computed the drift on the NVE simulations starting at 300 K from the same initial structure. Each simulation lasts 10 ps for both DFTB3/3OB and DFTB3/3OB-dDMC. The result shows that the approximate gradient does not influence the energy conservation since both methods show a critical drift for a time step of 2.4 fs.

The simulations on the caffeine-receptor complex[70–72] are conducted in the NVT ensemble using the Langevin thermostat with a 2 ps^{-1} friction. We found that a 1 fs time step is small enough to avoid energy drifts. The so-called "reference structure", optimized at the PBE0-dDsC/def2-SVP[70] level was taken as the initial structure for the DFTB3/3OB simulations. A snapshot of the DFTB3/3OB trajectory after 5 ps was taken as the starting structure for the PBE-dDsC simulation. All trajectories were thermalized for 5 ps at their respective level.

Results

The following illustrates the performance of dDMC not only on interaction energies of static dimer structures but especially on practical examples featuring geometry optimizations and molecular dynamics simulations.

Figure 1 displays the mean absolute error of the dDMC correction applied to DFTB3/3OB and PM6 compared to the uncorrected variants and the -D3 corrected energies.

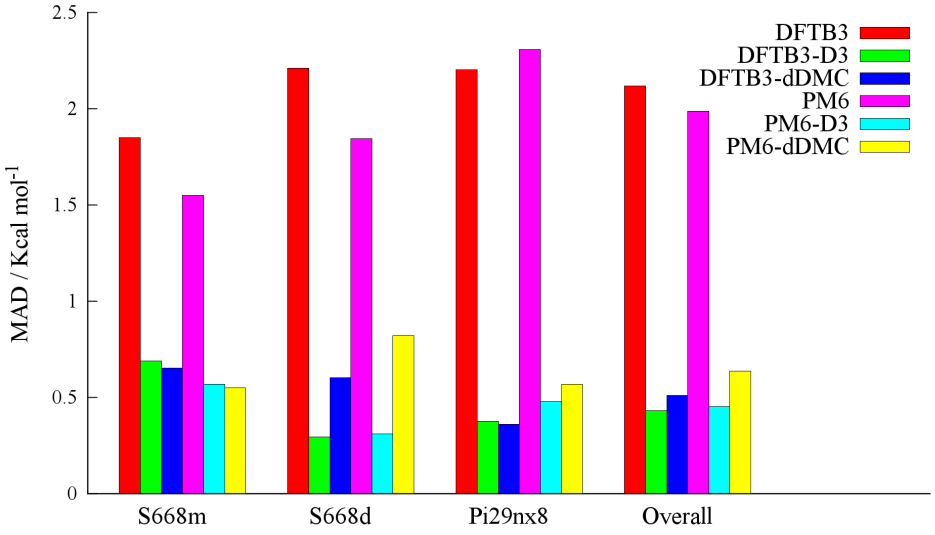

Figure 1: Mean absolute error of DFTB3/3OB[42] and PM6 and the D3[48,73] and dDMC dispersion corrected variants. The "overall" data set displays the MAD of all the dataset together.

Overall, the mean absolute errors for the DFTB3 corrected energies are below 0.7 kcal mol^{-1}. Despite its simplicity, the performance of -dDMC is very similar to –D3 except for the S66*8d subset that is notably better described at the DFTB3-D3 level (MAD = 0.29 kcal mol^{-1}). The poorer performance of dDMC for this specific subset essentially arises from an overbinding of the hydrogen-rich dimers such as those made of aliphatic chains (e.g., neopentane, pentane as seen in the SI). The present focus is essentially placed on π-π stacking but the combination of –dDMC with a H4[48] type correction that contains a specific repulsive term to correct the interaction between hydrogen atoms would surely improve the results for these complexes. The superior performance of DFTB3-dDMC as compared to PM6-dDMC is rooted in the less reliable Mulliken charges associated with the PM6 Hamiltonian.[64] Besides the reasonable performance, a clear benefit of using the dDMC scheme is certainly the gain in computational speed, which is especially visible when computing the gradients on large-scale systems (80% faster than the DFTD3 program version 2.1 rev 3 in calculating gradients on around 1000 atoms, see Supplementary Materials).

The authors recently demonstrated that the original DFTB3/MIO11[44] parameters lead to spurious energies and geometries for any systems that features a sulfur atom involved in a non-covalent interaction.[45] As illustrated by the examples provided in Figure 2, the latest 3OB parameterization

247 by Cui *et al.*[41,42] offers a dramatic improvement over MIO11 for the dispersion corrected gas phase
248 geometries. DFTB/3OB-dDMC leads to four geometries that are in close agreement with the
249 reference PBE0-dDsC/def2-SVP[71] or RI-MP2/TZ[74–76] data. In particular, the T-shape thiophene
250 dimer and the illustrative caffeine-receptor comple[70,71] are well reproduced with both DFTB/3OB-
251 dDMC and DFTB/3OB-D3 (RMSD < 0.4 Å). The -D3 description of the annulated β-trithiophene
252 dimer[45,77] converges toward another minima (RMSD= 2.025 Å), whereas dDMC remains in
253 agreement with the reference data (RMSD = 0.6Å). Similar discrepancies are observed for the anti-
254 parallel thiophene dimer. Note that our training set placing more emphasis on improving the
255 treatment of sulfur interactions could be at the origin of this difference. While the spurious
256 overbinding characteristic of the non-dispersion corrected DFTB/MIO11 geometries is recurrent
257 and relatively large in magnitude (sometime even larger than the reference interaction energy), the
258 3OB parameters offer a significant improvement: the DFTB3/3OB optimized geometries still bind
259 but the interaction energies involved are nevertheless much smaller than the reference and
260 dispersion corrected values.

261

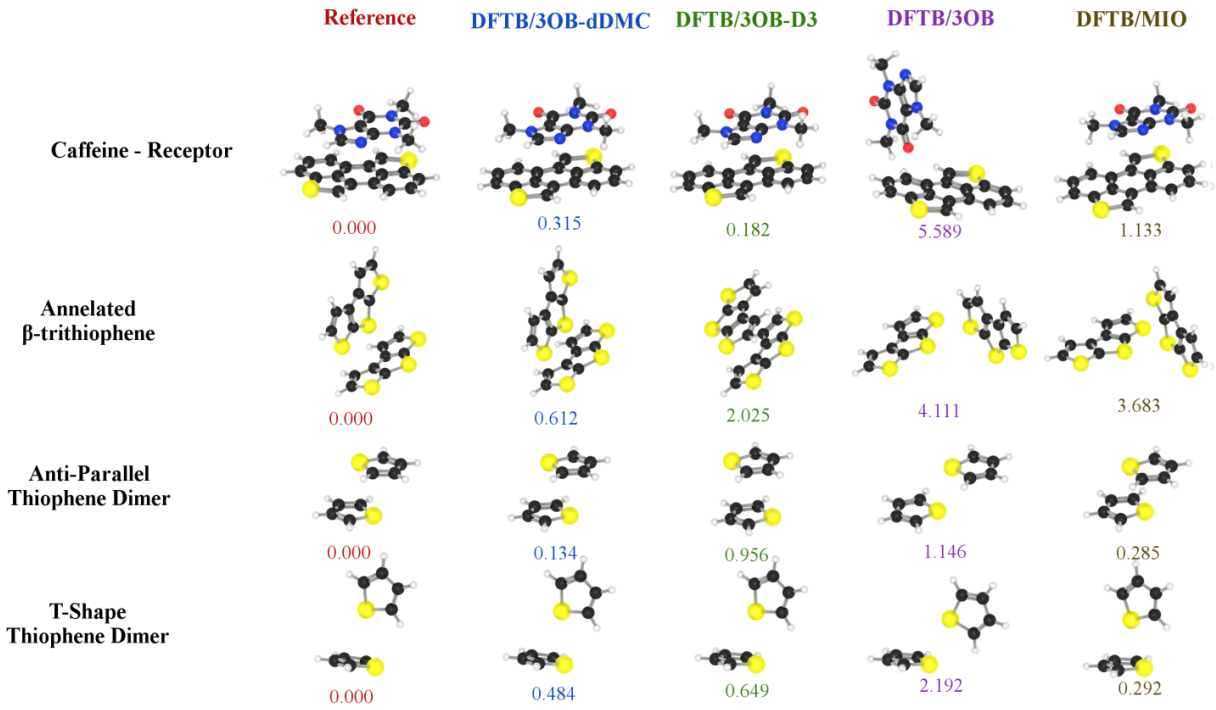

262

Figure 2: Comparisons of the DFTB geometry of sulfur-containing compounds geometries at both dispersion- (dDMC and D3) and non- corrected levels (with the 3OB and MIO parameters). RMSD (Å) with respect to the reference geometry are reported for each complex. The reference geometries of the caffeine-receptor and the annelated β-trithiopene[45,77] complexes are computed at the PBE0-dDsC/def2-SVP level.[71] The anti-parallel thiophene dimer system is optimized at the RI-MP2/TZ[74–76] level with Counter Poise correction to avoid BSSE[63] in Turbomole5.1.[78]

The performance of DFTB3/3OB-dDMC is further validated on the Born-Oppenheimer molecular dynamic simulations of two examples dominated by intra- and intermolecular interactions respectively. Figure 3 shows MD trajectories of an illustrative dithiacyclophane incorporating a thieno-[2,3-b]-thiophen that was originally chosen to evaluate the importance of self-consistency in dDsC.[69] This compound is rather challenging due to its large flexibility inherent to the existence of several low energy conformers featuring both π-π stacked and open conformations. We here present the molecular dynamic trajectories starting from two closed (i.e., π-π stacked) conformers (**A** and **B**) and monitor the distance between the barycentre of the benzene ring and the middle of the C-C bond of the thienothiophene ring over 8 ps trajectories that are directly compared to our former PBE-dDsC simulations taken from Corminboeuf and co-workers[69]. On average, the three tested dispersion-corrected schemes lead to very similar distances with no systematic over/underestimation: The average distance at the DFTB/3OB-dDMC level is the longest for the first trajectory (i.e., starting from conformer **A**) but the shortest for the second trajectory. The simulation of the closed conformer **B** performed at both non-corrected levels, PBE and DFTB/3OB, readily open. In contrast, the opening of conformer **A** differs significantly between PBE and DFTB/3OB. The PBE opening process is relatively sudden, whereas the DFTB/3OB structure opens more gradually. Other deviations observed between the non-corrected approaches include the larger flexibility of DFTB as compared to PBE.

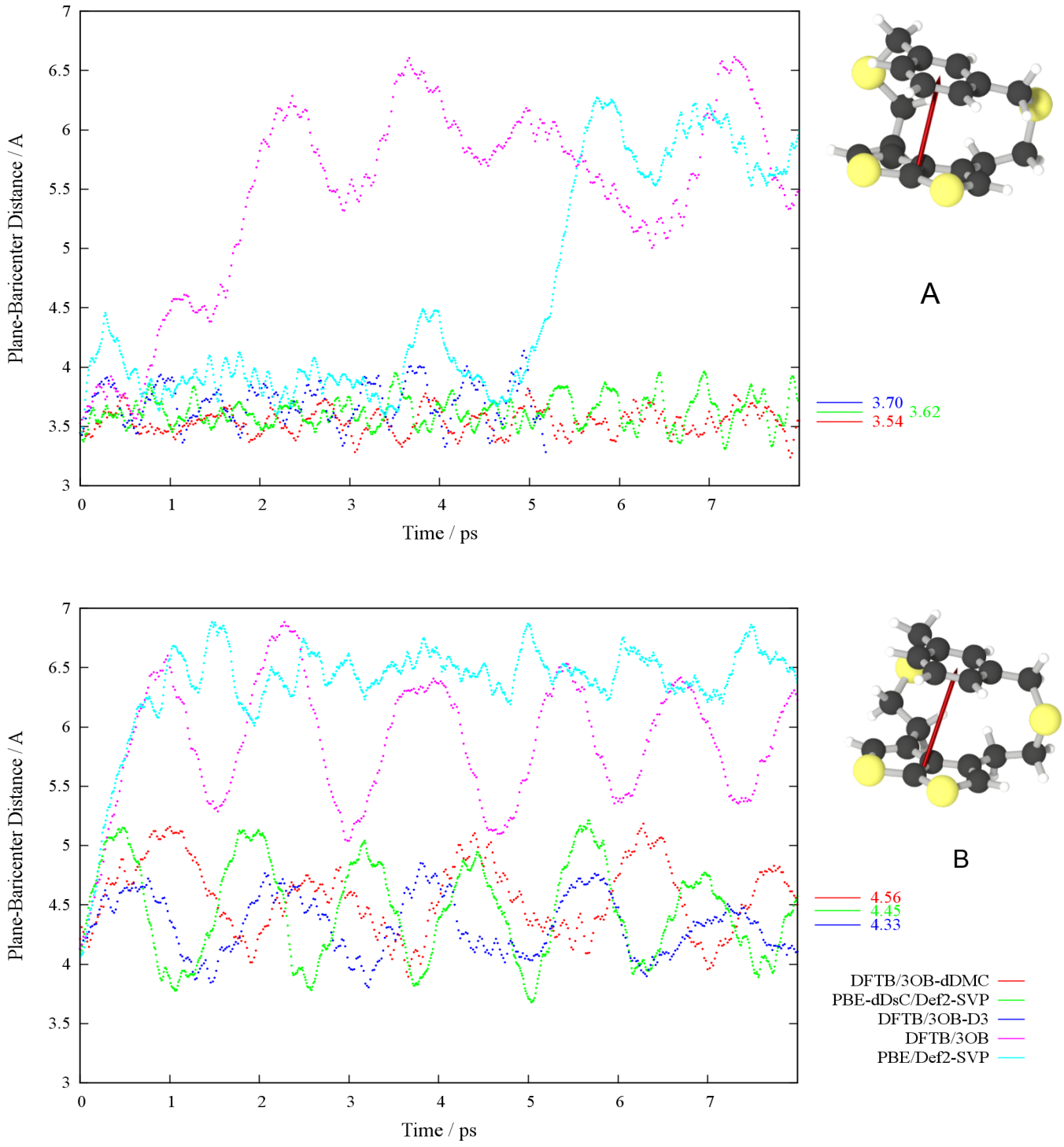

Figure 3: Profiles of the distance between the barycenter of the benzene ring and the middle of the C-C bond of the thienothiophene ring over a NVE Born-Oppenheimer molecular dynamic trajectory (see red arrow). Computations are performed at room temperature with non-corrected and dispersion corrected PBE and DFTB/3OB. The starting structure are optimized at ωB97X-D/6-31G* level[79–81]. The methods used to perform the simulations are distinguished by color.

The last molecular dynamics example (Figure 4) inspects the longer range intermolecular interaction of an illustrative caffeine-receptor dimer already studied in Refs[71,72] that is also included in our comparisons of geometry optimizations (Figure 2). The distance monitored is taken between a plane that best incorporates the atoms of the receptor and the barycenter of the caffeine molecule. The 350 ps DFTB3/3OB-dDMC trajectory is compared to that of DFTB3/3OB-dDMC and to a shorter 134.5 ps PBE-dDsC/def2-SVP trajectory. The histogram and overall trajectories show a nice correlation between the two DFTB/3OB corrected approaches correlate. The overall observation is that accounting for dispersion is ubiquitous when performing *ab initio* molecular dynamic trajectories. Our simulations also demonstrate that the residual error related to the 3OB sulfur parameters is counterbalance if combining DFTB/3OB with a dispersion correction. Within the framework of DFTB, dDMC represents a very simple and efficient alternative to the existing schemes specifically adapted to biomolecules for addressing problematic relevant to the field of organic electronic.

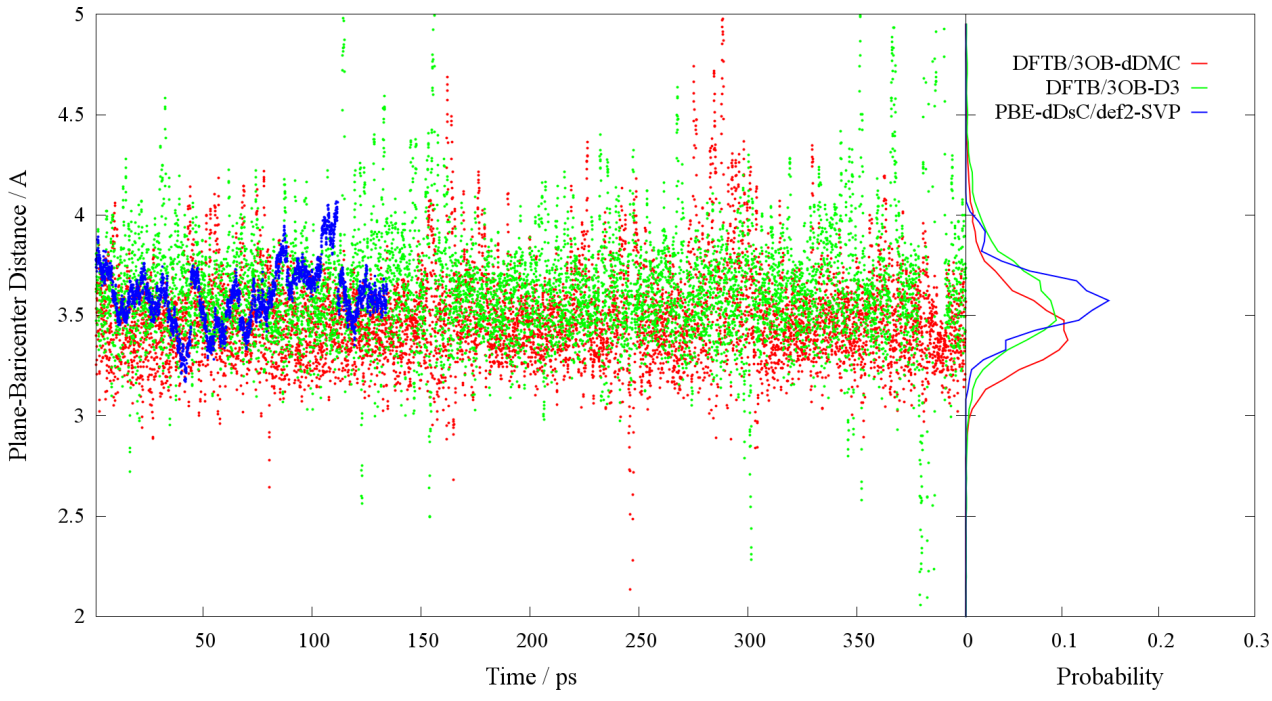

Figure 4: Profiles and histograms of the distance between the average plane of the receptor and the the barycentre of the caffeine over a NVT Born-Oppenheimer molecular dynamic trajectory.

Computations are performed at room temperature with DFTB3/3OB-dDMC, DFTB3/3OB-D3 and PBE-dDsC/def2-SVP.

Conclusions

This work introduces a fast atom-pairwise dispersion correction based on Mulliken charges that is specifically tailored for DFTB3. Unlike previous dispersion corrected DFTB computations focusing on biological systems, we here place a special emphasis on improving the description of compounds prevalent in the field of organic electronics. In this respect, the dDMC scheme performs especially well for the energies (MAD=0.7 kcal mol^{-1} for the test set of 94 compounds for a total of 752 different systems), geometries and molecular dynamics of sulfur-containing moieties involved in π-π stacking interactions that are known to be especially challenging for DFTB. We have thus provided both, a valuable extension to DFTB3 by providing a charge-dependent dispersion correction and a careful validation of the provided scheme on test sets for typical weak interactions (S66) and motives typical for organic electronics (Pi29).

The rising interest in organic electronic materials along with the simplicity of the proposed correction suggests that this approach has great potential. Future developments should enable the treatment of explicit solvent and the consideration of many body contributions that potentially play a role in determining the geometries and thermodynamics of nanoscale assemblies of organic molecules.

ACKNOWLEDGMENTS The author acknowledge Funding from the *European Research Council* (ERC Grants 306528, "COMPOREL").

SUPPORTING INFORMATION Additional Supporting Information may be found in the online version of this article.

Bibliography

(1) Allard, S.; Forster, M.; Souharce, B.; Thiem, H.; Scherf, U. *Angew. Chemie Int. Ed.* **2008**, *47*, 4070.

(2) Günes, S.; Neugebauer, H.; Sariciftci, N. S. *Chem. Rev.* **2007**, *107*, 1324.

(3) Walzer, K.; Maennig, B.; Pfeiffer, M.; Leo, K. *Chem. Rev.* **2007**, *107*, 1233.

(4) Joachim, C.; Gimzewski, J. K.; Aviram, A. *Nature* **2000**, *408*, 541.

(5) Kay, E. R.; Leigh, D. A.; Zerbetto, F. *Angew. Chemie Int. Ed.* **2007**, *46*, 72.

(6) Kinbara, K.; Aida, T. *Chem. Rev.* **2005**, *105*, 1377.

(7) Baldo, M. A.; O'Brien, D. F.; You, Y.; Shoustikov, A.; Sibley, S.; Thompson, M. E.; Forrest, S. R. *Nature* **1998**, *395*, 151.

(8) Borsenberger, P. M.; Fitzgerald, J. J. *J. Phys. Chem.* **1993**, *97*, 4815.

(9) Elstner, M.; Hobza, P.; Frauenheim, T.; Suhai, S.; Kaxiras, E. *J. Chem. Phys.* **2001**, *114*, 5149.

(10) Wu, X.; Vargas, M. C.; Nayak, S.; Lotrich, V.; Scoles, G. *J. Chem. Phys.* **2001**, *115*, 8748.

(11) Meijer, E. J.; Sprik, M. *J. Chem. Phys.* **1996**, *105*, 8684.

(12) Klimeš, J.; Michaelides, A. *J. Chem. Phys.* **2012**, *137*, 120901.

(13) Grimme, S. *Wiley Interdiscip. Rev. Comput. Mol. Sci.* **2011**, *1*, 211.

(14) Johnson, E. R.; Becke, A. D. *J. Chem. Phys.* **2005**, *123*, 024101.

(15) Tkatchenko, A.; Scheffler, M. *Phys. Rev. Lett.* **2009**, *102*, 073005.

(16) Sato, T.; Nakai, H. *J. Chem. Phys.* **2009**, *131*, 224104.

(17) Grimme, S.; Antony, J.; Ehrlich, S.; Krieg, H. *J. Chem. Phys.* **2010**, *132*, 154104.

(18) Steinmann, S. N.; Corminboeuf, C. *J. Chem. Theory Comput.* **2011**, *7*, 3567.

(19) Grimme, S. *J. Comput. Chem.* **2004**, *25*, 1463.

(20) Grimme, S. *J. Comput. Chem.* **2006**, *27*, 1787.

(21) Becke, A. D.; Johnson, E. R. *J. Chem. Phys.* **2005**, *123*, 154101.

(22) Becke, A. D.; Johnson, E. R. *J. Chem. Phys.* **2005**, *122*, 154104.

(23) DiStasio, R. *Proc. ...* **2012**, *109*, 14791.

(24) Al-Saidi, W. A.; Voora, V. K.; Jordan, K. D. *J. Chem. Theory Comput.* **2012**, *8*, 1503.

(25) Steinmann, S. N.; Csonka, G.; Corminboeuf, C. *J. Chem. Theory Comput.* **2009**, *5*, 2950.

(26) Steinmann, S. N.; Corminboeuf, C. *J. Chem. Theory Comput.* **2010**, *6*, 1990.

(27) Steinmann, S. N.; Corminboeuf, C. *J. Chem. Phys.* **2011**, *134*, 044117.

(28) Steinmann, S. N.; Corminboeuf, C. *Chimia (Aarau).* **2010**, *65*, 240.

(29) Hirshfeld, F. L. *Theor. Chim. Acta* **1977**, *44*, 129.

(30) Aradi, B.; Hourahine, B.; Frauenheim, T. *J. Phys. Chem. A* **2007**, *111*, 5678.

(31) Seifert, G.; Porezag, D.; Frauenheim, T. *Int. J. Quantum Chem.* **1996**, *58*, 185.

(32) Seifert, G. *J. Phys. Chem. A* **2007**, *111*, 5609.

(33) Seifert, G.; Eschrig, H.; Bieger, W. *ZEITSCHRIFT FUR Phys. CHEMIE-LEIPZIG* **1986**, *267*, 529.

(34) Elstner, M.; Porezag, D.; Jungnickel, G.; Elsner, J.; Haugk, M.; Frauenheim, T.; Suhai, S.; Seifert, G. *Phys. Rev. B* **1998**, *58*, 7260.

(35) Yang; Yu, H.; York, D.; Cui, Q.; Elstner, M. *J. Phys. Chem. A* **2007**, *111*, 10861.

(36) Gaus, M.; Cui, Q.; Elstner, M. *J. Chem. Theory Comput.* **2011**, *7*, 931.

(37) Barone, V.; Carnimeo, I.; Scalmani, G. *J. Chem. Theory Comput.* **2013**, *9*, 2052.

(38) Cui, Q.; Elstner, M.; Kaxiras, E.; Frauenheim, T.; Karplus, M. *J. Phys. Chem. B* **2001**, *105*, 569.

(39) McNamara, J. P.; Hillier, I. H. *Phys. Chem. Chem. Phys.* **2007**, *9*, 2362.

(40) Welke, K.; Watanabe, H. C.; Wolter, T.; Gaus, M.; Elstner, M. *Phys. Chem. Chem. Phys.* **2013**.

(41) Gaus, M.; Lu, X.; Elstner, M.; Cui, Q. *J. Chem. Theory Comput.* **2014**, *10*, 1518.

(42) Gaus, M.; Goez, A.; Elstner, M. *J. Chem. Theory Comput.* **2013**, *9*, 338.

(43) Krüger, T.; Elstner, M.; Schiffels, P.; Frauenheim, T. *J. Chem. Phys.* **2005**, *122*, 114110.

(44) Niehaus, T. A.; Elstner, M.; Frauenheim, T.; Suhai, S. *J. Mol. Struct. THEOCHEM* **2001**, *541*, 185.

(45) Petraglia, R.; Corminboeuf, C. *J. Chem. Theory Comput.* **2013**, *9*, 3020.

(46) Zhechkov, L.; Heine, T.; Patchkovskii, S.; Seifert, G.; Duarte, H. A. *J. Chem. Theory Comput.* **2005**, *1*, 841.

(47) Mulliken, R. *J. Chem. Phys.* **1955**, *23*, 1833.

(48) Řezáč, J.; Hobza, P. *J. Chem. Theory Comput.* **2011**, *8*, 141.

(49) Brandenburg, J. G.; Grimme, S. *J. Phys. Chem. Lett.* **2014**, *5*, 1785.

(50) Gonthier, J. F.; Steinmann, S. N.; Wodrich, M. D.; Corminboeuf, C. *Chem. Soc. Rev.* **2012**, *41*, 4671.

(51) Tang, K. T.; Toennies, J. P. *J. Chem. Phys.* **1984**, *80*, 3726.

(52) Tang, K. T.; Toennies, J. P.; Yiu, C. L. *Phys. Rev. Lett.* **1995**, *74*, 1546.

(53) Liu, Y.; Goddard, W. A. I. *Mater. Trans.* **2009**, *50*, 1664.

(54) Bondi, A. *J. Phys. Chem.* **1964**, *68*, 441.

(55) Rowland, R. S.; Taylor, R. *J. Phys. Chem.* **1996**, *100*, 7384.

(56) *Handbook of Chemistry and Physics (95th Edition)*; 2014.

(57) Goyal, P.; Elstner, M.; Cui, Q. *J. Phys. Chem. B* **2011**, *115*, 6790.

(58) Goyal, P.; Qian, H.-J.; Irle, S.; Lu, X.; Roston, D.; Mori, T.; Elstner, M.; Cui, Q. *J. Phys. Chem. B* **2014**, *118*, 11007.

(59) Řezáč, J.; Riley, K. E.; Hobza, P. *J. Chem. Theory Comput.* **2011**, *7*, 2427.

(60) Steinmann, S. N.; Corminboeuf, C. *J. Chem. Theory Comput.* **2012**, *8*, 4305.

(61) Halkier, A.; Helgaker, T.; Jørgensen, P.; Klopper, W.; Koch, H.; Olsen, J.; Wilson, A. K. *Chem. Phys. Lett.* **1998**, *286*, 243.

(62) Helgaker, T.; Klopper, W.; Koch, H.; Noga, J. *J. Chem. Phys.* **1997**, *106*, 9639.

(63) Boys, S. F.; Bernardi, F. *Mol. Phys.* **1970**, *19*, 553.

(64) Stewart, J. J. P. *J. Mol. Model.* **2007**, *13*, 1173.

(65) Bahn, S. R.; Jacobsen, K. W. *Comput. Sci. Eng.* **2002**, *4*, 56.

(66) Dolgonos, G.; Aradi, B.; Moreira, N. H.; Frauenheim, T. *J. Chem. Theory Comput.* **2010**, *6*, 266.

(67) Stewart, J. J. P. MOPAC 2012, 2012.

(68) Shao, Y.; Molnar, L. F.; Jung, Y.; Kussmann, J.; Ochsenfeld, C.; Brown, S. T.; Gilbert, A. T. B.; Slipchenko, L. V; Levchenko, S. V; O'Neill, D. P.; DiStasio, R. A.; Lochan, R. C.; Wang, T.; Beran, G. J. O.; Besley, N. A.; Herbert, J. M.; Lin, C. Y.; Van Voorhis, T.; Chien, S. H.; Sodt, A.; Steele, R. P.; Rassolov, V. A.; Maslen, P. E.; Korambath, P. P.; Adamson, R. D.; Austin, B.; Baker, J.; Byrd, E. F. C.; Dachsel, H.; Doerksen, R. J.; Dreuw, A.; Dunietz, B. D.; Dutoi, A. D.; Furlani, T. R.; Gwaltney, S. R.; Heyden, A.; Hirata, S.; Hsu, C.-P.; Kedziora, G.; Khalliulin, R. Z.; Klunzinger, P.; Lee, A. M.; Lee, M. S.; Liang, W.; Lotan, I.; Nair, N.; Peters, B.; Proynov, E. I.; Pieniazek, P. A.; Rhee, Y. M.; Ritchie, J.; Rosta, E.; Sherrill, C. D.; Simmonett, A. C.; Subotnik, J. E.; Woodcock, H. L.; Zhang, W.; Bell, A. T.; Chakraborty, A. K.; Chipman, D. M.; Keil, F. J.; Warshel, A.; Hehre, W. J.; Schaefer, H. F.; Kong, J.; Krylov, A. I.; Gill, P. M. W.; Head-Gordon, M. *Phys. Chem. Chem. Phys.* **2006**, *8*, 3172.

(69) Brémond, E.; Golubev, N.; Steinmann, S. N.; Corminboeuf, C. *J. Chem. Phys.* **2014**, *140*, 18A516.

(70) Gonthier, J. F.; Steinmann, S. N.; Roch, L.; Ruggi, A.; Luisier, N.; Severin, K.; Corminboeuf, C. *Chem. Commun.* **2012**, *48*, 9239.

(71) Luisier, N.; Ruggi, A.; Steinmann, S. *Org. Biomol. Chem.* **2012**, *10*, 7487.

(72) Rochat, S.; Steinmann, S. N.; Corminboeuf, C.; Severin, K. *Chem. Commun.* **2011**, *47*, 10584.

(73) Ehrlich, S.; Moellmann, J.; Reckien, W.; Bredow, T.; Grimme, S. *ChemPhysChem* **2011**, *12*, 3414.

(74) Weigend, F.; Häser, M. *Theor. Chem. Accounts Theory, Comput. Model. (Theoretica Chim. Acta)* **1997**, *97*, 331.

(75) Weigend, F.; Ahlrichs, R. *Phys. Chem. Chem. Phys.* **2005**, *7*, 3297.

(76) Schäfer, A.; Huber, C.; Ahlrichs, R. *J. Chem. Phys.* **1994**, *100*, 5829.

(77) Liu, H.; Kang, S.; Lee, J. Y. *J. Phys. Chem. B* **2011**, *115*, 5113.

(78) Turbomole V5.1 a development of University of Karlsruhe and Forschungszentrum Karlsuhe GmbH.

(79) Chai, J.-D.; Head-Gordon, M. *Phys. Chem. Chem. Phys.* **2008**, *10*, 6615.

(80) Chai, J.-D.; Head-Gordon, M. *J. Chem. Phys.* **2008**, *128*, 084106.

(81) Ditchfield, R. *J. Chem. Phys.* **1971**, *54*, 724.